Brain Topogr
DOI 10.1007/s10548-014-0386-2

ORIGINAL PAPER

Characterization of Post-traumatic Stress Disorder Using Resting-State fMRI with a Multi-level Parametric Classification Approach

Feng Liu · Bing Xie · Yifeng Wang · Wenbin Guo · Jean-Paul Fouche · Zhiliang Long · Wenqin Wang · Heng Chen · Meiling Li · Xujun Duan · Jiang Zhang · Mingguo Qiu · Huafu Chen

Received: 14 April 2014 / Accepted: 16 July 2014

Abstract Functional neuroimaging studies have found intra-regional activity and inter-regional connectivity alterations in patients with post-traumatic stress disorder (PTSD). However, the results of these studies are based on group-level statistics and therefore it is unclear whether PTSD can be discriminated at single-subject level, for instance using the machine learning approach. Here, we proposed a novel framework to identify PTSD using multi-level measures derived from resting-state functional MRI (fMRI). Specifically, three levels of measures were extracted as classification features: (1) regional amplitude of low-frequency fluctuations (univariate feature), which represents local spontaneous synchronous neural activity; (2) temporal functional connectivity (bivariate feature), which represents the extent of similarity of local activity between two regions, and (3) spatial functional connectivity (multivariate feature), which represents the extent of similarity of temporal correlation maps between two regions. Our method was evaluated on 20 PTSD patients and 20 demographically matched healthy controls. The experimental results showed that the features of each level could successfully discriminate PTSD patients from healthy controls. Furthermore, the combination of multi-level features using multi-kernel learning can further improve

Feng Liu and Bing Xie contributed equally to this work.

F. Liu · Y. Wang · Z. Long · H. Chen · M. Li · X. Duan · H. Chen (✉)
Key Laboratory for NeuroInformation of Ministry of Education, School of Life Science and Technology, University of Electronic Science and Technology of China, Chengdu 611054, Sichuan, People's Republic of China
e-mail: chenhf@uestc.edu.cn

F. Liu
Department of Radiology and Tianjin Key Laboratory of Functional Imaging, Tianjin Medical University General Hospital, Tianjin 300052, People's Republic of China

B. Xie
Department of Radiology, Southwest Hospital, Third Military Medical University, Chongqing 400038, People's Republic of China

B. Xie
Department of Anatomy, Third Military Medical University, Chongqing 400038, People's Republic of China

W. Guo
Mental Health Center, The First Affiliated Hospital, Guangxi Medical University, Nanning 410011, Guangxi, People's Republic of China

J.-P. Fouche
Department of Psychiatry, University of Cape Town, Cape Town 7925, South Africa

J.-P. Fouche
Department of Human Biology, University of Cape Town, Cape Town 7925, South Africa

J.-P. Fouche
Department of Psychiatry, University of Stellenbosch, Cape Town 7925, South Africa

W. Wang
School of Sciences, Tianjin Polytechnic University, Tianjin 300130, People's Republic of China

J. Zhang
School of Electrical Engineering and Information, Sichuan University, Chengdu 610065, People's Republic of China

M. Qiu
Department of Medical Image, College of Biomedical Engineering, Third Military Medical University, Chongqing 400038, People's Republic of China

Published online: 31 July 2014

the classification performance. Specifically, the classification accuracy obtained by the proposed framework was 92.5 %, which was an increase of at least 5 and 17.5 % from the two-level and single-level feature based methods, respectively. Particularly, the limbic structure and prefrontal cortex provided the most discriminant features for classification, consistent with results reported in previous studies. Together, this study demonstrated for the first time that patients with PTSD can be identified at the individual level using resting-state fMRI data. The promising classification results indicated that this method may provide a complementary approach for improving the clinical diagnosis of PTSD.

Keywords Temporal functional connectivity · Spatial functional connectivity · Multi-level feature · Multi-kernel learning · Limbic system · Prefrontal cortex

Introduction

Post-traumatic stress disorder (PTSD) is a highly disabling condition observed in individuals exposed to a traumatic event, such as war, violent crime and motor vehicle accidents. Among these traumas, motor vehicle accidents are the leading causes of PTSD (Chossegros et al. 2011). It has been found that individuals who were in an accident where medical attention was needed, an estimated 50 % of those developed PTSD (Blanchard and Hickling 2004). PTSD is characterized by persistent recall of the traumatic event, avoidance of any reminders of this trauma and hyperarousal (Yehuda and Flory 2007). Patients with PTSD suffer from enduring vigilance and sensitivity to environmental threat (van der Kolk 1989), and 19 % of patients will attempt suicide (Kessler 2000; Kessler et al. 1999). However, the diagnosis of PTSD to date is mainly based on assessment of signs and symptoms and a thorough psychological evaluation. Therefore, there has been substantial interest in assisting diagnosis of PTSD, by utilizing automated, unbiased methods.

Functional neuroimaging studies have demonstrated that PTSD is linked with local abnormalities in many brain regions, such as hippocampus (Astur et al. 2006), amygdala (Bryant et al. 2008), insula (Chen et al. 2009), superior frontal gyrus and middle temporal gyrus (Yin et al. 2012). Moreover, changes in functional connectivity have been found between specific region pairs in PTSD, such as decreased lingual-middle temporal gyrus connectivity (Qin et al. 2012), decreased amygdala-putamen connectivity (Linnman et al. 2011), increased amygdala-insula connectivity (Rabinak et al. 2011) and stronger basolateral amygdala-pregenual anterior cingulate cortex connectivity (Brown et al. 2014). These widespread differences indicate that abnormalities of brain function in PTSD not only relate to a single region but also to functional connectivity.

Although the aforementioned findings suggest brain functional changes in PTSD patients, there is limited application of these findings for clinical diagnosis. This is because all of these studies have used mass-univariate analytical methods that allow inference at the group level only. For neuroimaging to be useful in a clinical setting, one must be able to provide predictions at the individual level. In the past few years, the application of machine learning techniques to neuroimaging has made promising improvements in brain disease classification (Haller et al. 2014). Relative to traditional analyses based on group comparison, machine learning methods allow inference at the single-subject level rather than group level. Furthermore, machine learning approaches are sensitive to subtle and spatially distributed differences in the brain that might be undetectable using group comparison methods. Recently, a growing number of studies have applied machine learning methods on neuroimaging data to identify psychiatric disease (Liu et al. 2012a; Mourao-Miranda et al. 2012; Zeng et al. 2012). However, few studies have been conducted in PTSD.

There is ample evidence from previous functional neuroimaging studies that the spontaneous low frequency oscillations of the human brain measured with resting-state functional MRI (fMRI) are physiologically meaningful and relate to neural spontaneous activity (Biswal et al. 1995). Resting-state fMRI can provide two distinct types of information about brain function: segregation and integration. The regional amplitude of low-frequency fluctuations (ALFF), reflecting spontaneous neural activity during resting-state, can be used to explore regional neural function (Guo et al. 2012; Zang et al. 2007). Measures of functional connectivity at the temporal scale, reflecting the level of integration of that local activity across brain regions, can be utilized to improve the knowledge of brain networks (Greicius 2008). Therefore, investigation of the ALFF may advance our understanding of the functional segregation of the brain, while investigation on temporal connectivity patterns may increase our understanding of the functional integration within the brain (Sporns 2011). Additionally, functional connectivity at the spatial scale has been used to characterize the functional architecture of the human and monkey brain (Fox et al. 2006; Vincent et al. 2007). In contrast to the temporal correlation patterns obtained by measuring the extent of similarity of BOLD time series between two regions, spatial correlation patterns are obtained by measuring the extent of similarity of temporal correlation maps of the regions (He et al. 2009).

From the viewpoint above, ALFF, temporal connectivity and spatial connectivity can be considered as the different levels of the functional hierarchy. Recent studies have

demonstrated that integrating different levels of features can successfully classify brain disease (Dai et al. 2012; Sato et al. 2012) and combination of multi-level features can give better classification performance than single-level features. Traditionally, we can combine different levels of features by concatenating them into a long feature vector and then train a single classifier. However, the disadvantages of such concatenation are twofold. First, the concatenation method equally treats each level of features, without effectively exploring the complementary (different but useful) information carried by different feature levels. Second, the appropriate normalization (e.g., z-score standardization or scaled to range [-1, +1]) is needed for concatenating features extracted from different sources and, if not, the prediction might be easily dominated by a single feature type.

Motivated by issue above, a novel framework was proposed to differentiate PTSD patients from healthy controls. Specifically, ALFF, temporal connectivity patterns and spatial connectivity patterns were extracted from resting-state fMRI data and used as classification features. A hybrid feature selection method was then utilized at each feature level separately to select the optimal features for classification. Finally, a multi-kernel support vector machine (SVM) algorithm was employed to combine the selected features of each level for PTSD diagnosis. In the present study, our aims were firstly to examine whether ALFF, temporal connectivity patterns and spatial connectivity patterns would allow accurate discrimination between PTSD patients and healthy controls, and secondly, to investigate whether the complementary information conveyed among different feature levels can be integrated to improve classification performance.

Materials and Methods

Subjects

Twenty right-handed patients with PTSD who had been involved in a motor vehicle accident were recruited from the Southwest Hospital, Third Military Medical University, China. Six months following each participant's motor accident, the diagnosis of PTSD was made with the Clinician-Administered PTSD Scale for DSM-IV (CAPS-DX) (Blake et al. 1995). These subjects participated in this study within 1 month after diagnosis. Three main kinds of symptoms were assessed for both intensity and frequency, including the symptoms of re-experiencing, avoidant and increased arousal. A severity score for each symptom was computed by summing up the intensity and frequency scores, which were summed up for all 17 symptom questions and/or for the three symptoms. Exclusion criteria included suffering any brain injury in the motor vehicle accident, psychiatric co-morbidity (such as major depressive disorder and other anxiety disorders) which was assessed using the Structured Clinical Interview for DSM-IV (First et al. 1995), a history of neuropsychiatric disorders, a history of loss consciousness and alcohol or drug abuse. All patients had not taken psychotropic medication in the past 2 months. In addition, twenty right-handed healthy controls matched for age, gender and years of education were recruited from the community by advertisement. None of them had a history of psychiatric or neurological disorders, recent medication that might affect brain function and alcohol or drug abuse. This study was approved by the local ethical committee, and written informed consent was obtained from each subject.

Overview of Methodology

The proposed PTSD classification framework is shown in Fig. 1, which is summarized as follows:

1. After fMRI data preprocessing, ALFF map, temporal functional connectivity matrix and spatial functional connectivity matrix were calculated for each subject. Subsequently, these three levels of features were extracted from each subject.
2. For each feature level, we used a hybrid feature selection method which comprised *t* test and SVM-based feature selection to obtain the optimal subset of features.
3. Individual kernel matrices were computed from the selected features of each level and then combined to form a single mixed-kernel matrix.
4. The integrated mixed-kernel matrix was employed to train SVM classifiers and unbiased estimation of the classification performance was obtained via a nested cross-validation scheme.

MRI Data Acquisition

The fMRI images were acquired on a 3.0-T Siemens MRI scanner (Trio; Siemens Medical, Erlangen, Germany). During scanning, the subjects were instructed to keep their eyes closed, relax, and move as little as possible. Foam pads were used to minimize head movements and scanner noise. Functional sequences consisted of single-shot, echo-planar imaging (EPI) with repetition time (TR) = 2,000 ms, echo time (TE) = 30 ms, flip angle (FA) = 90°, matrix = 64 × 64, field of view (FOV) = 220 mm ×220 mm, slices = 36, slice thickness = 3 mm. For each participant, the fMRI scanning lasted for 6 min, and 180 volumes were obtained.

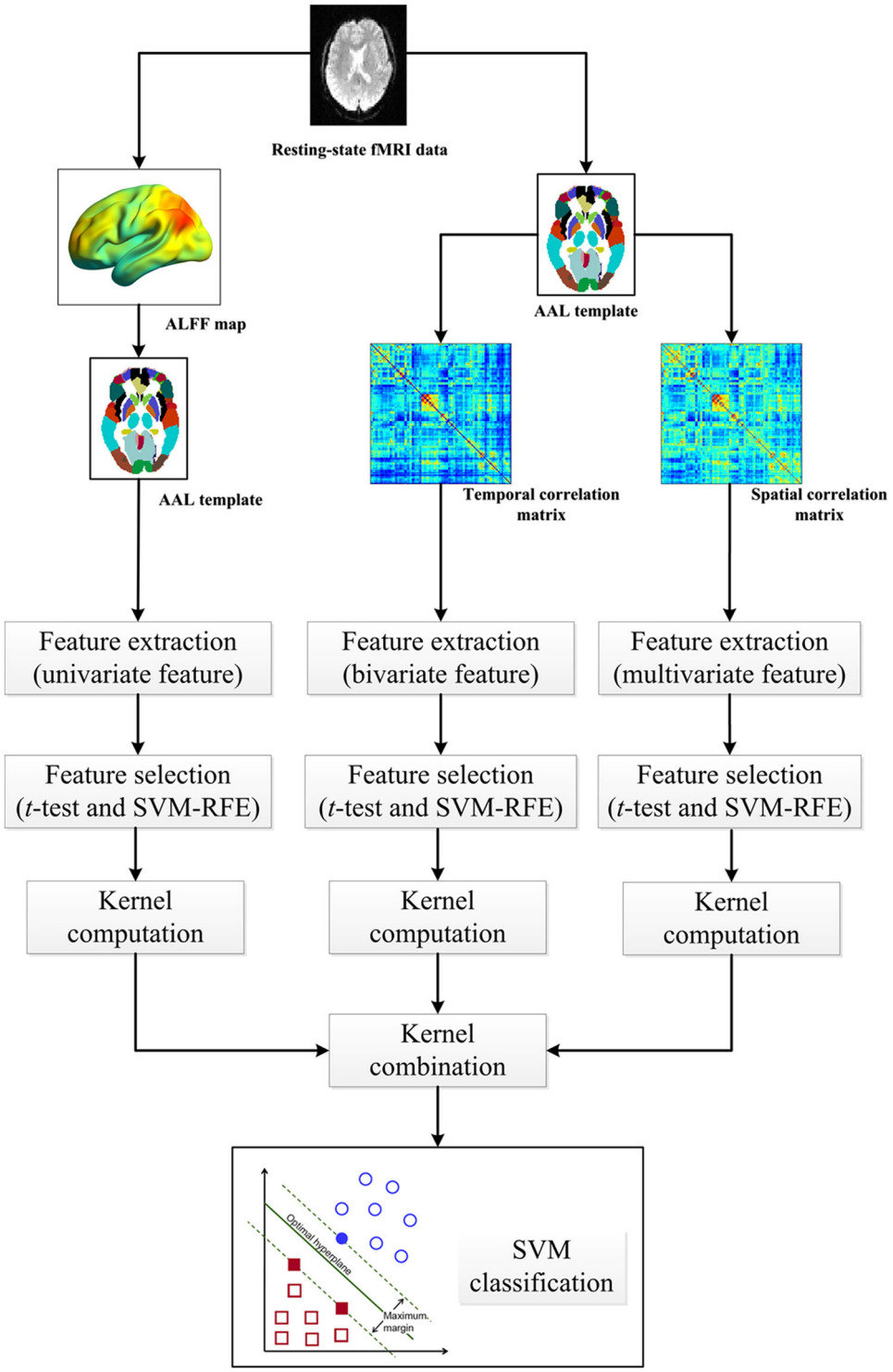

Fig. 1 Schematic diagram illustrating the proposed classification framework using multi-kernel SVM with multi-level features derived from resting-state functional MRI. *ALFF* amplitude of low-frequency fluctuations, *AAL* automated anatomical labeling, *SVM-RFE* support vector machine-recursive feature elimination

Data Preprocessing

Image preprocessing was performed with Data Processing Assistant for Resting-State fMRI (DPARSF) toolbox (Chao-Gan and Yu-Feng 2010). Briefly, the first 10 volumes of each subject were discarded to allow for magnetization equilibrium and the participants adapting to the scanning noise (Liu et al. 2013b). The remaining 170 volumes were corrected for the acquisition time delay between slices and then realigned to the first volume for the head motion correction. None of the participants was excluded according to the criterion of a displacement of more than 3 mm or an

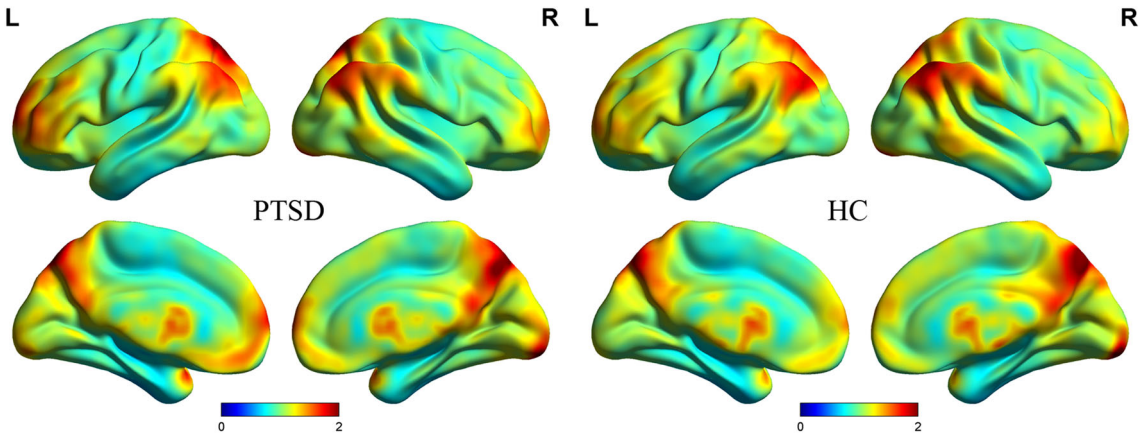

Fig. 2 Distribution of ALFF maps within groups. Mean ALFF maps within the patient group (*left*) and control group (*right*). The *color bar* represents the strength of ALFF. *PTSD* post-traumatic stress disorder, *HC* healthy control, *L* left, *R* right (Color figure online)

angular rotation of greater than 3° in any direction, as suggested by Wang et al. (2013). Moreover, the head motion profiles were matched between the PTSD and HC groups ($p > 0.135$ in any direction). The realigned images were spatially normalized to the Montreal Neurological Institute EPI template in SPM8 by combining affine transformation and non-linear deformations and resampled to $3 \times 3 \times 3$ mm^3.

ALFF

The normalized fMRI data were first spatially smoothed with an 8 mm full width at half maximum (FWHM) Gaussian kernel (Liu et al. 2012b). After linear-trend removal and band-pass filtering (0.01–0.08 Hz), we regressed six head motion parameters, white matter signal, cerebrospinal fluid signal and their first derivatives. The time series were then transformed into frequency domain using fast Fourier transformation and the power spectrum was estimated. Because the power of a given frequency is proportional to the square of the amplitude of the frequency component, the average square root of the power spectrum is taken as the ALFF (Zang et al. 2007; Zuo et al. 2010). For standardization purpose, the ALFF of each voxel was divided by the global mean ALFF value. The mean ALFF map of each group is presented in Fig. 2.

Functional Connectivity at the Temporal Scale

To construct large-scale brain functional connectivity at the temporal scale, the registered fMRI data were first divided into 116 anatomical regions of interest (ROIs) according to the automated anatomical labeling (AAL) atlas (Tzourio-Mazoyer et al. 2002). The regions in the AAL atlas were listed in Table 1. No spatial smoothing was applied in the preprocessing procedure in order to avoid introducing artificial local spatial correlations (Liu et al. 2013a). The mean time series of each ROI was obtained by averaging the time series of all voxels within that ROI. The time series were further linearly detrended and temporally band-pass filtered. The nuisance signals involving six head motion parameters, white matter signal, cerebrospinal fluid signal and their first derivatives were then regressed out from the data. It is still an ongoing controversy of removing the global signal in the calculation of resting-state functional connectivity (Fox et al. 2009; Murphy et al. 2009; Saad et al. 2012). Therefore, we did not regress out the global signal in this study. The residuals of these regressions were used for the following functional connectivity analysis. Finally, for each subject, a temporal correlation matrix was obtained by calculating the Pearson's correlation coefficients between the residual time series of each pair of regions as

$$r_{ab} = \frac{\sum_{t=1}^{T} [y_a(t) - \bar{y}_a] \cdot [y_b(t) - \bar{y}_b]}{\sqrt{\sum_{t=1}^{T} [y_a(t) - \bar{y}_a]^2} \sqrt{\sum_{t=1}^{T} [y_b(t) - \bar{y}_b]^2}} \quad (1)$$

where $y_a(t)$ and $y_b(t)$ $(t = 1, 2, \ldots, T; T = 170)$ were the residual time series of region a and b with means of $\bar{y}_a$ and $\bar{y}_b$, respectively. A Fisher's Z-transformation (Cohen et al. 2013) was applied on the elements of the correlation matrix to improve the normality as

$$z = \frac{1}{2}[\ln(1 + r) - \ln(1 - r)] \quad (2)$$

where r is the Pearson correlation coefficient and z is approximately a normal distribution. The mean temporal correlation matrix of each group is provided in Fig. 3.

Functional Connectivity at the Spatial Scale

The spatial functional connectivity between any two brain regions was computed as (He et al. 2009)

Table 1 The names and abbreviations of the AAL template

Index	Regions	Abbr.	Index	Regions	Abbr.
(1,2)	Precentral gyrus	PreCG	(63,64)	Supramarginal gyrus	SMG
(3,4)	Superior frontal gyrus	SFG	(65,66)	Angular gyrus	ANG
(5,6)	Superior frontal gyrus, orbital part	SFGorb	(67,68)	Precuneus	PCUN
(7,8)	Middle frontal gyrus	MFG	(69,70)	Paracentral lobule	PCL
(9,10)	Middle frontal gyrus, orbital part	MFGorb	(71,72)	Caudate nucleus	CAU
(11,12)	Inferior frontal gyrus, opercular part	IFGoper	(73,74)	Lenticular nucleus, putamen	PUT
(13,14)	Inferior frontal gyrus, triangular part	IFGtri	(75,76)	Lenticular nucleus, pallidum	PAL
(15,16)	Inferior frontal gyrus, orbital part	IFGorb	(77,78)	Thalamus	THA
(17,18)	Rolandic operculum	ROL	(79,80)	Heschl gyrus	HES
(19,20)	Supplementary motor area	SMA	(81,82)	Superior temporal gyrus	STG
(21,22)	Olfactory cortex	OLF	(83,84)	Temporal pole: superior temporal gyrus	TPOsup
(23,24)	Superior frontal gyrus, medial	SFGmed	(85,86)	Middle temporal gyrus	MTG
(25,26)	Superior frontal gyrus, medial orbital	SFGmorb	(87,88)	Temporal pole: middle temporal gyrus	TPOmid
(27,28)	Gyrus rectus	REC	(89,90)	Inferior temporal gyrus	ITG
(29,30)	Insula	INS	(91,92)	Cerebelum_Crus1	CERcr1
(31,32)	Anterior cingulate gyrus	ACG	(93,94)	Cerebelum_Crus2	CERcr2
(33,34)	Median cingulate gyrus	MCG	(95,96)	Cerebelum_3	CER3
(35,36)	Posterior cingulate gyrus	PCG	(97,98)	Cerebelum_4&5	CER4&5
(37,38)	Hippocampus	HIP	(99,100)	Cerebelum_6	CER6
(39,40)	Parahippocampal gyrus	PHG	(101,102)	Cerebelum_7	CER7
(41,42)	Amygdala	AMYG	(103,104)	Cerebelum_8	CER8
(43,44)	Calcarine fissure	CAL	(105,106)	Cerebelum_9	CER9
(45,46)	Cuneus	CUN	(107,108)	Cerebelum_10	CER10
(47,48)	Lingual gyrus	LING	109	Vermis_1&2	VER1&2
(49,50)	Superior occipital gyrus	SOG	110	Vermis_3	VER3
(51,52)	Middle occipital gyrus	MOG	111	Vermis_4&5	VER4&5
(53,54)	Inferior occipital gyrus	IOG	112	Vermis_6	VER6
(55,56)	Fusiform gyrus	FFG	113	Vermis_7	VER7
(57,58)	Postcentral gyrus	PoCG	114	Vermis_8	VER8
(59,60)	Superior parietal gyrus	SPG	115	Vermis_9	VER9
(61,62)	Inferior parietal lobule	IPL	116	Vermis_10	VER10

Odd and even numbers (1–108) represent brain regions of left and right hemispheres, respectively

AAL automated anatomical labeling

$$R_{ab} = \frac{\sum_{m=1,m\neq a,m\neq b}^{M}[z_a(m)-\bar{z}_a]\cdot[z_b(m)-\bar{z}_b]}{\sqrt{\sum_{m=1,m\neq a,m\neq b}^{M}[z_a(m)-\bar{z}_a]^2}\sqrt{\sum_{m=1,m\neq a,m\neq b}^{M}[z_b(m)-\bar{z}_b]^2}} \quad (3)$$

where $z_a(m)$ and $z_b(m)$ $(m = 1, 2, \ldots, M; m \neq a, m \neq b, M = 116)$ were the ath and bth columns of the temporal correlation matrix obtained above (after Fisher's Z-transformation) with means of $\bar{z}_a$ and $\bar{z}_b$, respectively. The spatial connectivity between two brain regions denotes the degree of similarity in the temporal connectivity patterns of the two regions. The Fisher's Z-transformation was also performed on the elements of the spatial connectivity matrix to improve the normality. The mean spatial correlation matrix of each group is shown in Fig. 4.

Feature Extraction

The ALFF map for each subject was parcellated into 116 ROIs based on the AAL atlas. The mean ALFF values of

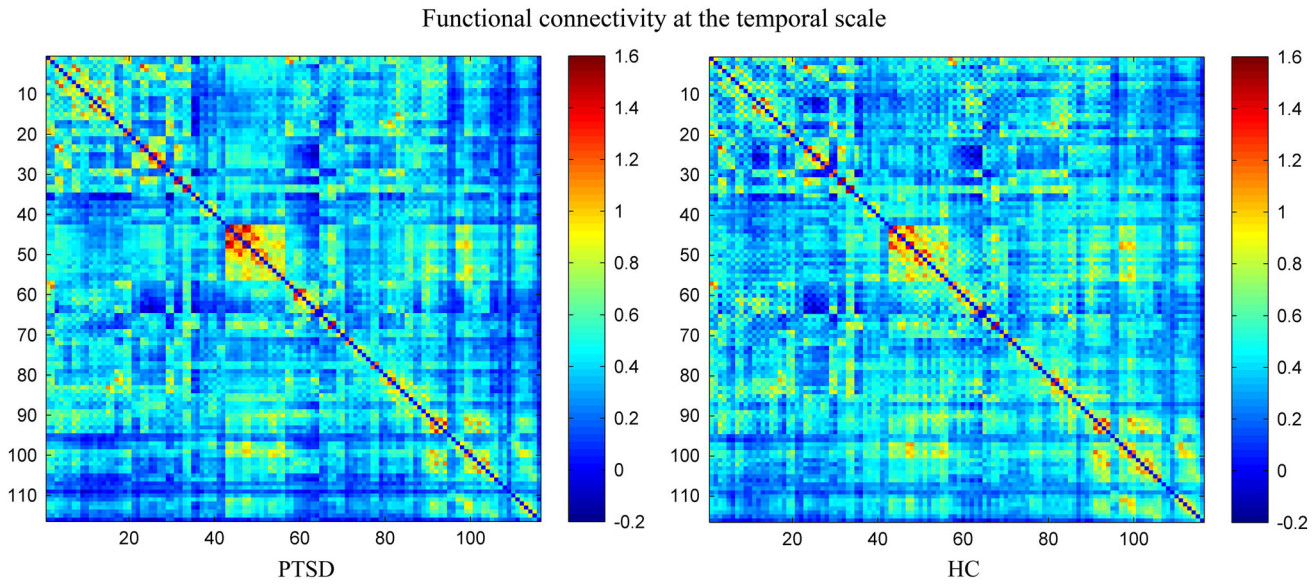

Fig. 3 Mean temporal functional connectivity matrix for patient group (*left*) and control group (*right*). The *color bar* represents the *z* value of temporal functional connectivity. *PTSD* post-traumatic stress disorder, *HC* healthy control (Color figure online)

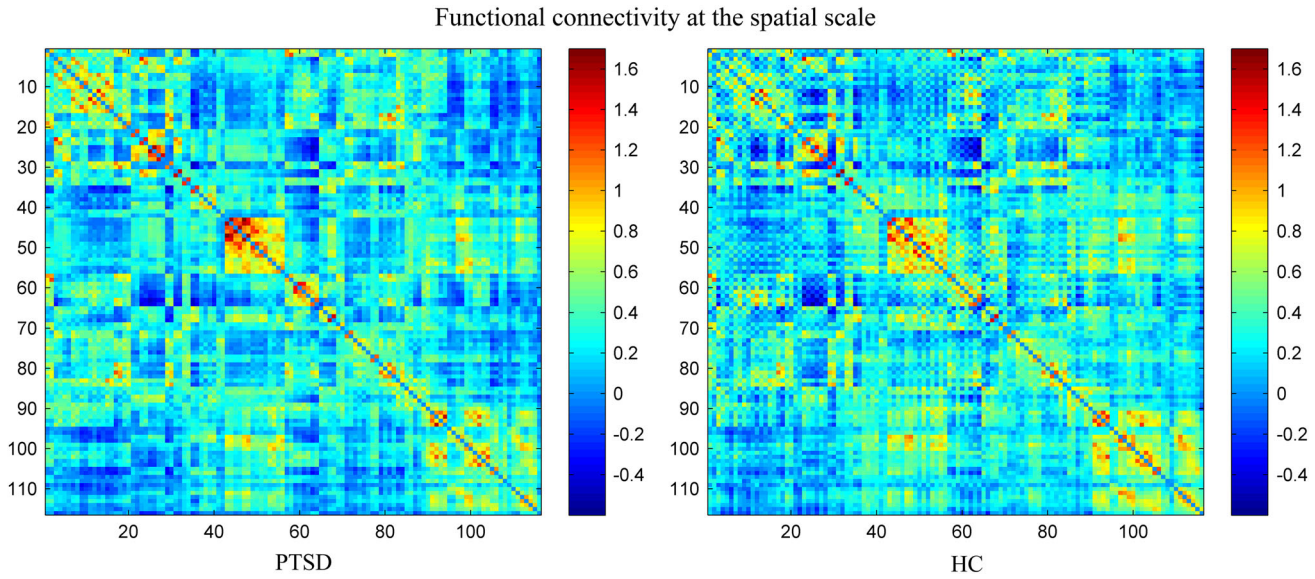

Fig. 4 Mean spatial functional connectivity matrix for patient group (*left*) and control group (*right*). The *color bar* represents the *z* value of spatial functional connectivity. *PTSD* post-traumatic stress disorder, *HC* healthy control (Color figure online)

all the ROIs were computed and considered as *univariate* features. In addition, we had a temporal/spatial functional connectivity map for each subject. Each map was represented by a 116 × 116 symmetric matrix. Removing 116 diagonal elements in each matrix, the upper triangle elements of the symmetric matrix were extracted and viewed as *bivariate/multivariate* features.

Feature Selection

The dimensionality of original features is much higher than the number of samples, which may lead to the "curse of dimensionality" problem and high computational complexity. Feature selection is a useful and important method to remove irrelevant or redundant features for dimensionality reduction and improving the performance of the classifier (Guyon and

Elisseeff 2003). We used a hybrid feature selection method, which combines filter- and wrapper-based approaches, to select the most relevant features for PTSD classification. Specifically, in the filter-based approach, only features with a p value smaller than the predefined threshold ($p < 0.05$, uncorrected), measured by a two-sample t test, were retained for subsequent feature selection. Despite the reduction in dimensionality of feature space, the filter-based approach was performed independently for each feature, ignoring the relationship (redundant or complementary) with other features. This may cause some redundant features to be selected and influence the classification performance. To avoid this problem, we employed a wrapper-based method named SVM-recursive feature elimination [SVM-RFE (Guyon et al. 2002)] for further feature selection, which jointly considers the discriminative power among features. The aim of SVM-RFE is to find a subset of features to reduce the classification error. This hybrid feature selection method was performed separately on each feature level. For each feature level, we finally have an individual optimal feature subset. Of note, all the procedures of feature selection were constrained to the training set, without using the information of the test set, in order to avoid the introduction of bias.

Multi-kernel SVM

In order to effectively integrate multi-level feature vectors, multi-kernel SVM was used in this study (Liu et al. 2014). In brief, after the feature selection procedure mentioned above, we constructed a kernel matrix for each feature level, and then combined them using a weighted linear combination as follows:

$$K\left[\left(\mathbf{x}_n^1, \mathbf{x}_n^2, \mathbf{x}_n^3\right), \left(\mathbf{x}^1, \mathbf{x}^2, \mathbf{x}^3\right)\right] = \sum_{f=1}^{3} \beta^f k^f\left(\mathbf{x}_n^f, \mathbf{x}^f\right) \tag{4}$$

where $\left(\mathbf{x}_n^1, \mathbf{x}_n^2, \mathbf{x}_n^3\right)$ is the feature vectors of the nth sample with three levels of features $\mathbf{x}_n^1$, $\mathbf{x}_n^2$ and $\mathbf{x}_n^3$, and $\left(\mathbf{x}^1, \mathbf{x}^2, \mathbf{x}^3\right)$ is the feature vectors of a testing sample. $\beta^f \geq 0$ is the weighting factor of f feature type with the constraint of $\sum_{f=1}^{3} \beta^f = 1$.

$k^f\left(\mathbf{x}_n^f, \mathbf{x}^f\right) = \phi^f\left(\mathbf{x}_n^f\right)^T \phi^f\left(\mathbf{x}^f\right)$ is the kernel function for samples $\mathbf{x}_n^f$ and $\mathbf{x}^f$, and ϕ^f is a kernel-induced mapping function of the f feature type. After constructing the integrated kernel matrix, it is then straightforward to apply a linear SVM as follows:

$$l(\mathbf{x}^1, \mathbf{x}^2, \mathbf{x}^3) = \operatorname{sign}\left\{\sum_{n=1}^{N} c_n \alpha_n K\left[\left(\mathbf{x}_n^1, \mathbf{x}_n^2, \mathbf{x}_n^3\right), \left(\mathbf{x}^1, \mathbf{x}^2, \mathbf{x}^3\right)\right] + b\right\} \tag{5}$$

where $c_n \in \{1, -1\}$ is the class label of the nth training sample, N is the total number of training samples, α_n is a Lagrangian multiplier, and b is a bias.

Cross-Validation

Support vector machine classifier with linear kernel was implemented via the LIBSVM toolbox (Chang and Lin 2011), with a default value for the parameter C (i.e., $C = 1$). A nested leave-pair-out cross-validation strategy was employed to evaluate the performance of the classifier, which could obtain a relatively unbiased estimation of the true generalization performance (Ecker et al. 2010; Mourao-Miranda et al. 2012). In each trial, we first excluded a demographically relatively matched pair of subjects (i.e., one to one matching, one subject from each group) to comprise the test set, then performed a second split where we repeatedly repartitioned the remaining 19 subject pairs into a validation set (1 pair) and training set (18 pairs). This procedure is repeated until all subject pairs have been left out for test. The optimal SVM model and optimal feature subset were obtained in the inner cross-validation before applying it to the test set. Accuracy, sensitivity, specificity and area under receiver operating characteristic curve (AUC) were adopted to evaluate the performance of the classifier based on the results of nested cross-validation.

$$\text{Accuracy} = \frac{\text{TP} + \text{TN}}{\text{TP} + \text{FN} + \text{TN} + \text{FP}} \tag{6}$$

$$\text{Sensitivity} = \frac{\text{TP}}{\text{TP} + \text{FN}} \tag{7}$$

$$\text{Specificity} = \frac{\text{TN}}{\text{TN} + \text{FP}} \tag{8}$$

where TP, TN, FP and FN denote true positive, true negative, false positive and false negative, respectively. In addition, other statistical measures were further used to evaluate the diagnostic power of the proposed method. The Youden's index (YOI), positive predictive value (PPV) and negative predictive value (NPV) were defined as (Altman and Bland 1994; Sokolova et al. 2006)

$$\text{PPV} = \frac{\text{TP}}{\text{TP} + \text{FP}} \tag{9}$$

$$\text{NPV} = \frac{\text{TN}}{\text{TN} + \text{FN}} \tag{10}$$

$$\text{YOI} = \frac{\text{TP}}{\text{TP} + \text{FN}} + \frac{\text{TN}}{\text{TN} + \text{FP}} - 1 \tag{11}$$

The PPV, also termed precision rate, is the proportion of positive test results which are true positives. The NPV reflects the proportion of subjects with a negative test result who are correctly diagnosed. The YOI evaluates the ability of a classifier to avoid failure by equally weighting its performance on positive and negative samples.

Permutation Testing

Permutation testing was performed to derive a p value to determine whether classification accuracy exceeded chance

Table 2 Demographics and clinical characteristics of patients with PTSD and HC

Variables (mean ± SD)	PTSD	HC	*p* value
Gender (M/F)	20 (13/7)	20 (14/6)	0.74[a]
Handedness (right/left)	20/0	20/0	–
Age (years)	32.92 ± 8.48	31.53 ± 7.43	0.45[b]
Education (years)	11.20 ± 3.80	13.00 ± 2.20	0.37[b]
IQ	98.20 ± 5.50	103.20 ± 6.30	0.24[b]
CAPS total score	52.33 ± 9.44	8.26 ± 9.31	<0.01[b]

SD standard deviation, *PTSD* post-traumatic stress disorder, *HC* healthy controls, *IQ* intelligence quotient, *CAPS* clinician-administered PTSD scale (range 0–136)

[a] The *p* value was obtained by Chi square test

[b] The *p* values were obtained by two-sample *t* tests

levels (50 %). To this end, the class labels were permuted 1,000 times (randomly assigning patient and control labels to the training subjects) and repeated for the entire cross-validation procedure. The *p* value was calculated as the proportion of accuracies that are equal to or greater than the one obtained by the real labels. If less than 5 % ($p < 0.05$) of the accuracies from all permutations was equal to or exceeded the non-permutated value, the result was deemed significant.

Results

Demographics and Clinical Characteristics of the Participants

Two-sample *t* tests were performed to assess the differences in age, years of education, intelligence quotient (IQ) score and clinical score, while Chi square test was performed to assess the difference in gender. The two groups were matched for gender (13 males for PTSD group and 14 males for control group; $p = 0.74$), age (32.92 ± 8.48 years for PTSD group; 31.53 ± 7.43 years for control group; $p = 0.45$), years of education (11.20 ± 3.80 years for PTSD group; 13.00 ± 2.20 years for control group; $p = 0.37$) and IQ value (98.20 ± 5.50 for PTSD group; 103.20 ± 6.30 for control group; $p = 0.24$). Compared with healthy controls, patients with PTSD have significantly higher CAPS total score. The detailed demographic and clinical data are shown in Table 2.

Experiment Settings

In our experiments, the proposed framework was compared with six other classification approaches which used different levels of features: (1) univariate feature; (2) bivariate feature; (3) multivariate feature; (4) combination of univariate and bivariate features; (5) combination of univariate and multivariate features; (6) combination of bivariate and multivariate features. Of note, we adopted the traditional single-kernel SVM classifier for classification using single level of features and multi-kernel SVM classifier for classification using two levels of features. It was also worth noting that the same training and test data were used in all methods for fair comparison.

Comparison of Classification Performance

As seen in Table 3, our proposed method obtained better performance than any of other six methods in all performance measures. Specifically, our method achieved a classification accuracy of 92.5 % ($p < 0.001$), a sensitivity of 90 %, a specificity of 95 %, a PPV of 94.7 %, an NPV of 90.5 %, a YOI of 0.85 and an AUC of 0.91. In contrast, for the single-level feature method, the best accuracy was only 75 % ($p < 0.003$) and for the two-level feature method, the best accuracy was 87.5 % ($p < 0.001$). The improvement in classification performance indicated the superiority of the proposed framework in better characterizing the brain functional anomalies in PTSD patients. We also evaluated the classification performance by direct feature concatenation. Specifically, 116 univariate features from ALFF, 6,670 bivariate features from temporal functional connectivity and 6,670 multivariate features from spatial functional connectivity were concatenated into a long feature vector. Subsequently, the same feature selection and cross-validation procedure were performed, and traditional single-kernel SVM classifier was used to evaluate the classification performance. As shown in Table 3, the classification accuracy was 77.5 % and the AUC value was 0.83, which was worse than our framework. In the current study, we used a leave-pair-out cross-validation approach to evaluate the performance of the classifier, and the same training and test data were used in all methods for fair comparison. Thus, it would be interesting to see whether the same subjects were correctly classified across different feature levels. As shown in Table 4, the misclassified subjects were not the same across the univariate, bivariate and multivariate features, suggesting that the complementary information existed among these features.

The Most Discriminative Features

The most discriminative features that were selected using the proposed framework for PTSD classification were investigated. Since the feature selection in each fold was performed based on the training set, the selected features differ across different cross-validation folds. Thus, we defined the most discriminative features as features which were most frequently selected in all cross-validations. The

Table 3 Classification performance using different levels of features

Feature types	*p* value	ACC (%)	SEN (%)	SPE (%)	PPV (%)	NPV (%)	YOI	AUC
Univariate	<0.010	70.0	65.0	75.0	72.2	68.2	0.40	0.64
Bivariate	<0.004	72.5	70.0	75.0	73.7	71.4	0.45	0.77
Multivariate	<0.003	75.0	75.0	75.0	75.0	75.0	0.50	0.77
Univariate + bivariate	<0.001	82.5	80.0	85.0	84.2	81.0	0.65	0.83
Univariate + multivariate	<0.001	80.0	85.0	75.0	77.3	83.3	0.60	0.84
Bivariate + multivariate	<0.001	87.5	80.0	95.0	94.1	82.6	0.75	0.86
Concatenate	<0.001	77.5	80.0	75.0	76.2	79.0	0.55	0.83
Proposed	<0.001	92.5	90.0	95.0	94.7	90.5	0.85	0.91

Univariate feature = ALFF; bivariate feature = functional connectivity at the temporal scale; multivariate feature = functional connectivity at the spatial scale. The plus sign indicates the combination of two given types of features. "Concatenate" means all three feature levels were concatenated into a long feature vector. The *p* values were obtained by permutation tests

ACC accuracy, *SEN* sensitivity, *SPE* specificity, *PPV* positive predictive value, *NPV* negative predictive value, *YOI* Youden's index, *AUC* area under receiver operating characteristic curve, *ALFF* amplitude of low-frequency fluctuations

Table 4 Classification performance of each method per fold

Fold	U	B	M	U + B	U + M	B + M	C	P
1	100	100	100	100	100	100	100	100
2	50	100	100	100	100	100	100	100
3	100	0	100	50	100	100	100	100
4	100	100	100	100	100	100	100	100
5	50	100	50	100	50	100	50	100
6	50	100	100	100	100	100	100	100
7	50	50	100	50	100	100	50	100
8	0	50	50	50	50	50	50	50
9	50	50	0	100	50	50	50	100
10	50	100	100	100	100	100	100	100
11	50	100	50	100	50	100	50	100
12	100	0	0	50	50	0	0	50
13	100	50	100	50	100	100	100	100
14	50	100	100	100	100	100	100	100
15	100	100	100	100	100	100	100	100
16	100	100	100	100	100	100	100	100
17	100	100	100	100	100	100	100	100
18	50	50	50	50	50	100	50	100
19	50	0	50	50	50	50	50	50
20	100	100	50	100	50	100	100	100

Univariate feature = ALFF; bivariate feature = functional connectivity at the temporal scale; multivariate feature = functional connectivity at the spatial scale. The plus sign indicates the combination of two given types of features. Of note, we used leave-pair-out cross-validation and the same training and test data were used in all methods for fair comparison. Thus, there are two subjects in the test set per fold. The number 0, 50, 100 (%) is the accuracy obtained by the corresponding method

U univariate, *B* bivariate, *M* multivariate, *U* + *B* univariate + bivariate, *U* + *M* univariate + multivariate, *B* + *M* bivariate + multivariate, *C* concatenate, *P* proposed

top fifteen selected univariate, bivariate and multivariate features are provided in Figs. 5, 6, 7. It is observed that the selected univariate features are from both brain hemispheres and all four lobes, indicating the widespread regional abnormalities over whole brain in PTSD patients. Based on the selected univariate features, the regions that contribute for accurate PTSD classification mainly included the bilateral median cingulate gyrus, bilateral orbitofrontal cortex, bilateral temporal pole, right amygdala, right inferior parietal lobule, right supplementary motor area, left postcentral gyrus, left calcarine fissure and right cerebellum. It can also be observed that the discriminative bivariate and multivariate features that contribute for classification are not only restricted within the same lobe or hemisphere but also across different lobes and hemispheres. This indicated that the connections between different areas of the brain, either adjacent or distant, might provide some meaningful information for describing the neurobiological underpinnings of PTSD symptoms. Based on the selected bivariate and multivariate features, most of the connections were associated with the prefrontal cortex.

Discussion

This study demonstrated for the first time that patients with PTSD can be discriminated from healthy controls using multi-level features extracted from resting-state fMRI data. The classification performance was evaluated via a nested leave-pair-out cross-validation strategy to ensure the generalization of the classifier. In agreement with our first hypothesis, each level of features can successfully discriminate PTSD patients from healthy controls. The best classification accuracy achieved by single-level method was 75 %. In contrast, the obtained results showed that our proposed framework can improve the classification performance by using a multi-kernel learning approach to fuse multi-level features. Specifically, our method achieved a high classification accuracy of 92.5 % ($p < 0.001$) for

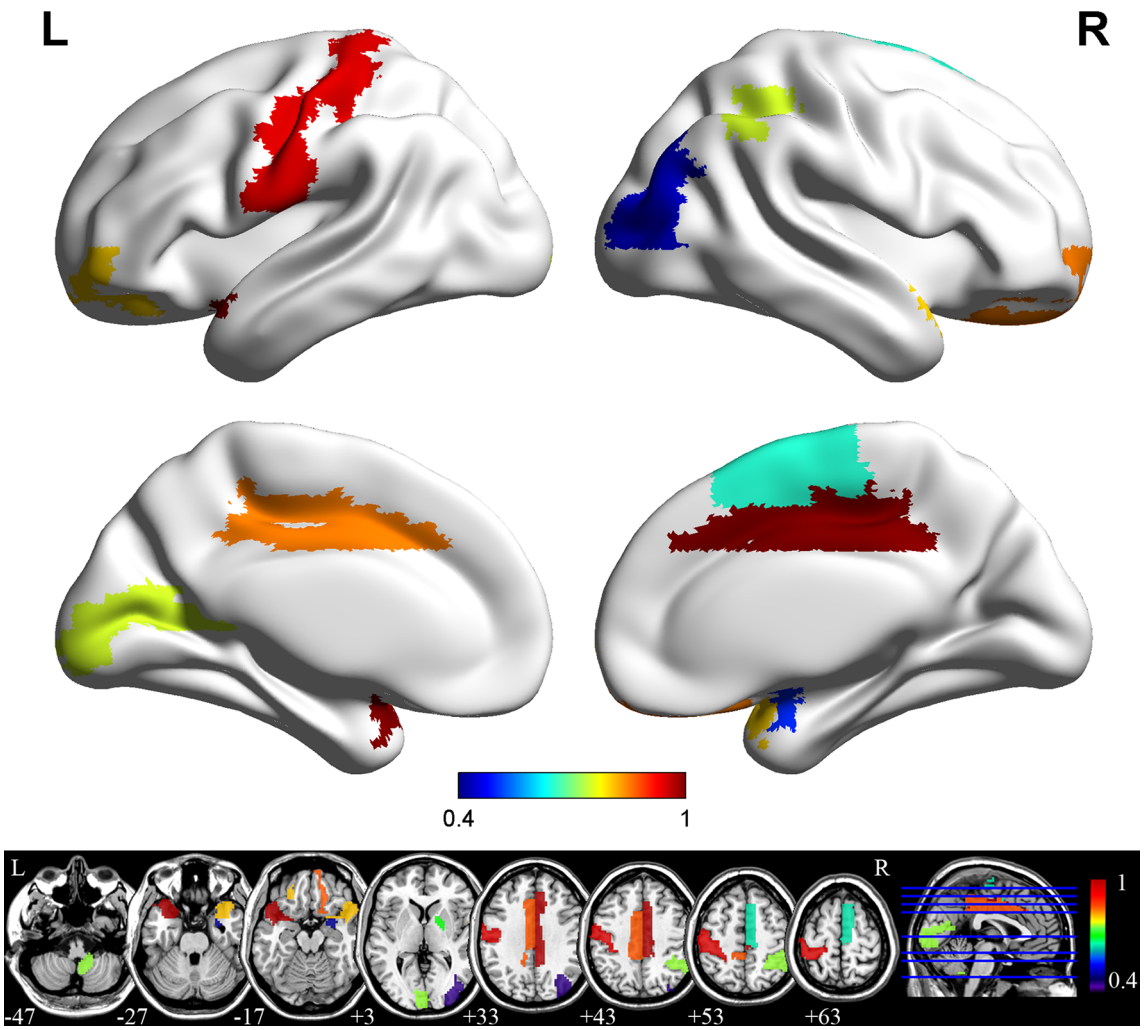

Fig. 5 The most discriminative univariate features (regional ALFF). To better represent the relative contribution of brain regions for classification, the regions were projected onto the cortical surface (*top*) and shown in 2D slice images (*down*). The *color* represents the feature weight (normalized selection frequency, i.e., the ratio of the actual number of selection times divided by the maximum possible number of selection times (always selected to form the final feature set in each cross-validation iteration)) for each ROI. The surface maps were visualized using BrainNet Viewer (Xia et al. 2013) and 2D slice map was made by using MRIcron (http://www.mccauslandcenter.sc.edu/mricro/mricron/). *L* left, *R* right (Color figure online)

PTSD classification and the AUC value was 0.91, indicating good discriminatory ability. These results suggested that single-level features could only afford limited information for classifying PTSD from controls, as indicated by the much smaller accuracy. However, information from different levels of features complements each other and potentially improves prediction accuracy. It's worth noting that combining biomarkers from different feature types with different data fusion methods to identify disease is still an open area of research. Our study demonstrated that multi-level features with multi-kernel learning can be used to discriminate PTSD patients with a relatively high accuracy.

In recent years, machine learning methods have been used extensively to identify brain disease and have obtained promising results (Liu et al. 2013c; Suk et al. 2013; Wee et al. 2014; Westman et al. 2013). Relative to the conventional methods based on group comparison, these kinds of methods allow inferences at the individual level rather than the group, and therefore yielding results with a potentially high level of clinical translation. Most importantly, machine learning approaches have the advantage of taking into account the relationship among features. Therefore, they are sensitive to spatially distributed and subtle differences in the brain, which may otherwise be undetectable using traditional univariate methods that focus on gross differences at group level. As shown in Figs. 2, 3, 4, visual examination suggests that the distributions of three levels of features are remarkably similar between groups in spite of some differences in

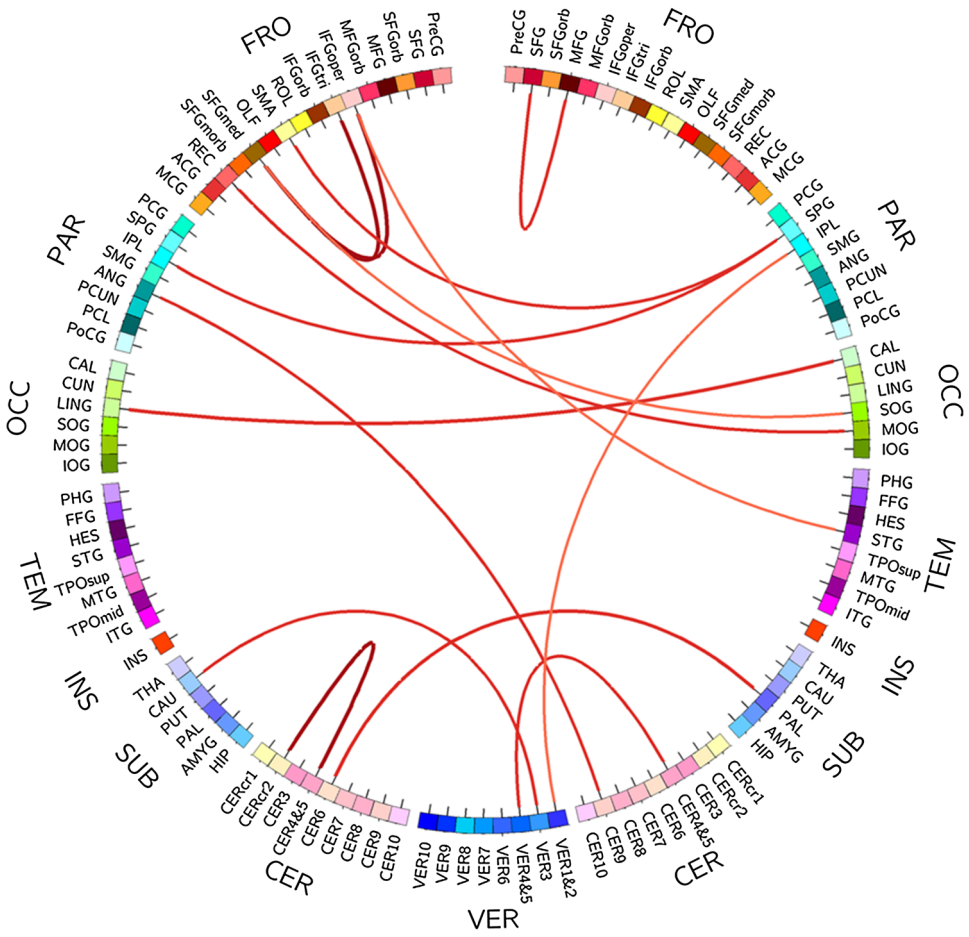

Fig. 6 Connectogram of the most discriminative bivariate features (temporal functional connectivity). Of note, the *left part* of the figure represents the left hemisphere and the *right part* of the figure represents the right hemisphere of the brain. *Thickness of each line* reflects its selection frequency, i.e., a *thicker line* indicates a higher selection frequency. *FRO* frontal lobe, *PAR* parietal lobe, *OCC* occipital lobe, *TEM* temporal lobe, *SUB* subcortical regions, *CER* cerebellum hemisphere, *VER* vermis. The other abbreviations can be found in Table 1

strength. For example, those regions with higher ALFF of two groups are primarily located in the bilateral medial prefrontal regions as well as lateral parietal regions and occipital regions. Classification results showed that regional ALFF could be used to successfully classify PTSD patients with an accuracy of 70 % ($p < 0.01$). This indicates that machine learning method has good potential to find subtle differences between two groups.

The most discriminative univariate features that were selected using the proposed approach for identifying the PTSD patients are reported. Regions, which are associated with the selected univariate features, are widespread and not restricted to particular brain hemispheres or lobes. These regions have been investigated before and are thought to be associated with PTSD, including the cingulate gyrus (Lanius et al. 2002; Tuescher et al. 2011), orbitofrontal cortex (Croy et al. 2010; Yan et al. 2013), temporal pole (Jatzko et al. 2006), amygdala (El Khoury-Malhame et al. 2011; Shin et al. 2006; Zantvoord et al. 2013), postcentral gyrus (Lindemer et al. 2013), inferior parietal lobule (Morey et al. 2008; Yin et al. 2012), cerebellum (Bing et al. 2013), pallidum (Long et al. 2013), calcarine fissure (Molina et al. 2010), occipital cortex (Chao et al. 2012) and supplementary motor area (Shaw et al. 2009). The fact that our experimental results are consistent with these previous studies demonstrates the efficacy of the proposed framework in identifying biomarkers for PTSD classification. It is interesting to observe that several regions in the limbic system have been selected as discriminative features. The limbic system is a group of interconnected cortical and subcortical regions which is primarily responsible for regulating human emotions as well as the formation of memories (Mega et al. 1997). In addition, this system has widespread connections to extensive cortical areas known as the neuroanatomical circuits of mood regulation, including the orbitofrontal cortex, cingulate gyrus, amygdala and so on (Catani et al. 2013). Recent studies have found that dysfunctions of the limbic regions are associated with emotion dysregulation in PTSD patients (Etkin and Wager 2007; Lanius et al. 2010). Therefore, these findings suggest that functional alterations in the limbic system are closely associated with the pathophysiology of PTSD.

Although a considerable body of evidence has accumulated over recent years on the regional dysfunction in PTSD, limited studies have investigated the changes in

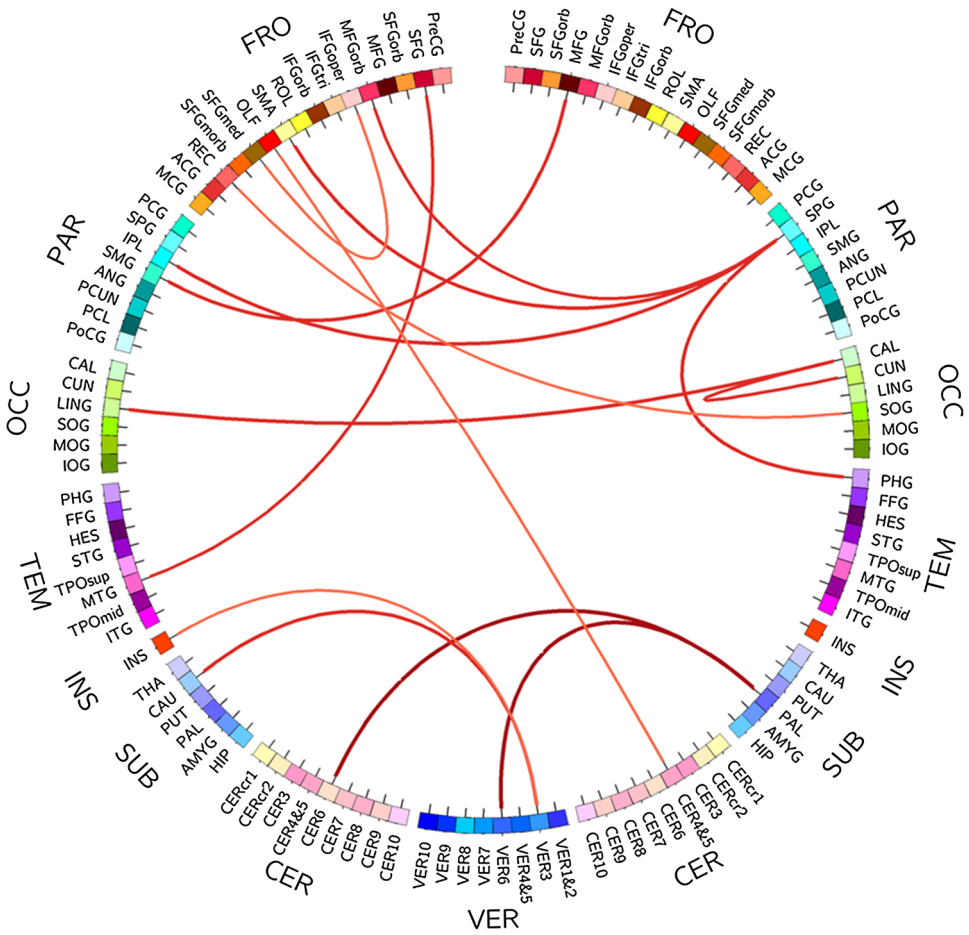

Fig. 7 Connectogram of the most discriminative multivariate features (spatial functional connectivity). Of note, the *left part* of the figure represents the left hemisphere and the *right part* of the figure represents the right hemisphere of the brain. *Thickness of each line* reflects its selection frequency, i.e., a *thicker line* indicates a higher selection frequency. *FRO* frontal lobe, *PAR* parietal lobe, *OCC* occipital lobe, *TEM* temporal lobe, *SUB* subcortical regions, *CER* cerebellum hemisphere, *VER* vermis. The other abbreviations can be found in Table 1

functional interaction between brain regions in PTSD patients during the resting state, which may provide complementary yet crucial information for better understanding of the pathophysiology of PTSD. In this study, we used both temporal and spatial functional connectivity as classification features and thus examined the alterations of functional connectivity in a comprehensive way. As shown in Figs. 6, 7, the most discriminative temporal and spatial connections have similar patterns. The selected bivariate and multivariate features mainly involve the prefrontal cortex, which is in line with a recently published study (Jin et al. 2014). The prefrontal cortex is known to be a key structure in the processes of body regulation, fear modulation and working memory (Braun 2011). Abnormal prefrontal cortex connectivity may lead to behavioral and cognitive control changes existed in PTSD.

In this study, we used both temporal functional connectivity and spatial functional connectivity as classification features. Since the calculation of the spatial connectivity pattern is based on the temporal connectivity pattern, there seems to be largely overlapped information among these two kinds of features. However, a number of recent studies have demonstrated that spatial correlation pattern is also an indispensable tool to investigate human brain. Two examples were given here for illustrating the importance of the functional connectivity at the spatial scale. First, the two core regions, ventromedial prefrontal cortex (VMPFC) and posterior cingulate cortex (PCC), of default mode network are highly functionally correlated in the sense of temporal functional connectivity (Fox et al. 2005). However, the spatial functional connectivity between VMPFC and PCC may not be so strong. Although the positively correlated networks for these two regions are largely overlapped, the negatively correlated networks for each showed striking differences (Uddin et al. 2009). Second, Margulies and colleagues have found that different subdivisions of precuneus have distinct patterns of functional connectivity at the temporal scale (Margulies et al. 2009). Specifically, the anterior part of the precuneus exhibits functional connectivity with paracentral lobule, motor cortex and superior parietal cortex; the central part shows functional connectivity to dorsomedial prefrontal, dorsolateral prefrontal and multimodal lateral inferior parietal cortex; the posterior part functionally connects with adjacent visual cortical regions. Thus, both temporal and spatial functional connectivity should be used to

comprehensively investigate the functional connectivity of the brain.

In addition to classification features, the method that combines the different types of features is also an important aspect for classification problem. In traditional classification methods, different types of features are usually concatenated into a longer feature vector. However, these methods may not be sufficiently effective for combining different types of features. In the current study, a multi-kernel learning approach was utilized to integrate different types of features. Hinrichs et al. (2009) have demonstrated that multi-kernel learning can effectively integrate different types of features. The main advantage of multi-kernel learning is that it offers more flexibility by using different weights on different types of features. This approach may provide us with a convenient way to combine different types of features for classification.

Several limitations should be noted. First, this study was limited by a relatively small sample size, which may limit the translational value of our results. Although cross-validation strategy was used to evaluate the performance of classification method, independent and multi-center imaging datasets should be used to confirm our results in the future. Second, we used resting-state fMRI data to extract classification features. Although resting-state fMRI is a promising technique for measuring spontaneous brain activity, it lacks direct observation of anatomical connections. Future studies may benefit from the combination of resting-state fMRI and diffusion MRI data. Third, previous studies have demonstrated that head motions a substantial impact on functional connectivity and other resting-state measures (Power et al. 2012; Satterthwaite et al. 2012; Van Dijk et al. 2012; Zeng et al. 2014). Although we controlled for head motion, we could not fully remove this effect. Future studies require systematic methodological work on this issue. Fourth, the whole brain was parcellated into 116 regions based on the AAL atlas. Recent studies have found that different parcellation schemes generated different results (Hayasaka and Laurienti 2010; Wang et al. 2009; Zalesky et al. 2010). Thus, it would be useful to determine which brain parcellation strategy is more appropriate to discriminate patients with PTSD in the future. Fifth, as our study only included patients who experienced motor vehicle accidents, we urge caution when generalizing these results to other traumatic events. Finally, we did not assess the depression and anxiety severity of the enrolled patients with the Hamilton Depression Scale (HAMD) and Hamilton Anxiety Scale (HAMA). However, we assessed the severity of these two symptoms with Symptom Checklist 90 (SCL-90) scale (Derogatis et al. 1976). The results indicated that the patients had only mild depression and anxiety symptoms. Moreover, depression and anxiety might be the inherent symptoms which could not be excluded from the analyses. Therefore, we did not use the severity of these two symptoms as covariates in the analyses.

Conclusion

In summary, the current study proposed a novel classification framework to separate patients with PTSD from demographically matched healthy controls using multi-level features derived from resting-state fMRI scans. Compared with the single- and two-level methods, improvement in classification performance was obtained by integrating the three-level features via multi-kernel learning. Moreover, the discriminative selected univariate features for accurate classification were generally consistent with previous studies, particularly components in the limbic structure, indicating the ability of our framework in determining PTSD disease-associated biomarkers. Furthermore, the selected bivariate and multivariate features showed similar patterns of association with the prefrontal cortex, indicating behavioral and cognitive control changes in PTSD. These promising classification results provide evidence of the effectiveness of this framework for potentially improving the clinical diagnosis of PTSD. Future studies may benefit from the integration of diffusion MRI or other imaging modalities as well as genetic and clinical information.

Acknowledgments The authors thank the three anonymous reviewers for the constructive suggestions. This work was supported by the 973 project (2012CB517901), the Natural Science Foundation of China (Nos. 61125304, 61035006, 61273361, 30870696 and 81301279), the China Scholarship Council (No. 2011607033), the Scholarship Award for Excellent Doctoral Student granted by Ministry of Education (No. A03003023901010), the Fundamental Research Funds for the Central Universities (ZYGX2013Z004), the Specialized Research Fund for the Doctoral Program of Higher Education of China (No. 20120185110028), the Starting Fund of Third Military University (TMMU2009XHG01), Natural Science Foundation of Chongqing (CSTC2009BB5019) and the Key Technology R&D Program of Sichuan Province (2012SZ0159, Science & Technology Department of Sichuan Province).

Conflict of interest All authors declare that they have no conflicts of interest.

References

Altman DG, Bland JM (1994) Statistics notes: diagnostic tests 2: predictive values. BMJ 309:102

Astur RS, St Germain SA, Tolin D, Ford J, Russell D, Stevens M (2006) Hippocampus function predicts severity of post-traumatic stress disorder. Cyberpsychol Behav 9:234–240

Bing X, Ming-Guo Q, Ye Z, Jing-Na Z, Min L, Han C, Yu Z, Jia-Jia Z, Jian W, Wei C, Han-Jian D, Shao-Xiang Z (2013) Alterations in the cortical thickness and the amplitude of low-frequency fluctuation in patients with post-traumatic stress disorder. Brain Res 1490:225–232

Biswal B, Zerrin Yetkin F, Haughton VM, Hyde JS (1995) Functional connectivity in the motor cortex of resting human brain using echo-planar mri. Magn Reson Med 34:537–541

Blake DD, Weathers FW, Nagy LM, Kaloupek DG, Gusman FD, Charney DS, Keane TM (1995) The development of a clinician-administered PTSD scale. J Trauma Stress 8:75–90

Blanchard EB, Hickling EJ (2004) After the crash: psychological assessment and treatment of survivors of motor vehicle accidents. American Psychological Association, Washington, DC

Braun K (2011) The prefrontal–limbic system: development, neuroanatomy, function, and implications for socioemotional development. Clin Perinatol 38:685–702

Brown VM, LaBar KS, Haswell CC, Gold AL, McCarthy G, Morey RA (2014) Altered resting-state functional connectivity of basolateral and centromedial amygdala complexes in posttraumatic stress disorder. Neuropsychopharmacology 39:351–359

Bryant RA, Felmingham K, Kemp A, Das P, Hughes G, Peduto A, Williams L (2008) Amygdala and ventral anterior cingulate activation predicts treatment response to cognitive behaviour therapy for post-traumatic stress disorder. Psychol Med 38:555–561

Catani M, Dell'acqua F, Thiebaut de Schotten M (2013) A revised limbic system model for memory, emotion and behaviour. Neurosci Biobehav Rev 37:1724–1737

Chang C-C, Lin C-J (2011) LIBSVM: a library for support vector machines. ACM Trans Intell Syst Technol 2:27

Chao LL, Lenoci M, Neylan TC (2012) Effects of post-traumatic stress disorder on occipital lobe function and structure. NeuroReport 23:412–419

Chao-Gan Y, Yu-Feng Z (2010) DPARSF: a MATLAB toolbox for "pipeline" data analysis of resting-state fMRI. Front Syst Neurosci 4:13

Chen S, Li L, Xu B, Liu J (2009) Insular cortex involvement in declarative memory deficits in patients with post-traumatic stress disorder. BMC Psychiatry 9:39

Chossegros L, Hours M, Charnay P, Bernard M, Fort E, Boisson D, Sancho P-O, Yao SN, Laumon B (2011) Predictive factors of chronic post-traumatic stress disorder 6 months after a road traffic accident. Accid Anal Prev 43:471–477

Cohen J, Cohen P, West SG, Aiken LS (2013) Applied multiple regression/correlation analysis for the behavioral sciences. Routledge, London

Croy I, Schellong J, Joraschky P, Hummel T (2010) PTSD, but not childhood maltreatment, modifies responses to unpleasant odors. Int J Psychophysiol 75:326–331

Dai Z, Yan C, Wang Z, Wang J, Xia M, Li K, He Y (2012) Discriminative analysis of early Alzheimer's disease using multi-modal imaging and multi-level characterization with multi-classifier (M3). Neuroimage 59:2187–2195

Derogatis LR, Rickels K, Rock AF (1976) The SCL-90 and the MMPI: a step in the validation of a new self-report scale. Br J Psychiatry 128:280–289

Ecker C, Marquand A, Mourao-Miranda J, Johnston P, Daly EM, Brammer MJ, Maltezos S, Murphy CM, Robertson D, Williams SC, Murphy DG (2010) Describing the brain in autism in five dimensions—magnetic resonance imaging-assisted diagnosis of autism spectrum disorder using a multiparameter classification approach. J Neurosci 30:10612–10623

El Khoury-Malhame M, Reynaud E, Soriano A, Michael K, Salgado-Pineda P, Zendjidjian X, Gellato C, Eric F, Lefebvre MN, Rouby F, Samuelian JC, Anton JL, Blin O, Khalfa S (2011) Amygdala activity correlates with attentional bias in PTSD. Neuropsychologia 49:1969–1973

Etkin A, Wager TD (2007) Functional neuroimaging of anxiety: a meta-analysis of emotional processing in PTSD, social anxiety disorder, and specific phobia. Am J Psychiatry 164:1476–1488

First MB, Spitzer RL, Gibbon M, Williams JB (1995) The structured clinical interview for DSM-III-R personality disorders (SCID-II). Part II: multi-site test–retest reliability study. J Pers Disord 9:92–104

Fox MD, Snyder AZ, Vincent JL, Corbetta M, Van Essen DC, Raichle ME (2005) The human brain is intrinsically organized into dynamic, anticorrelated functional networks. Proc Natl Acad Sci USA 102:9673–9678

Fox MD, Corbetta M, Snyder AZ, Vincent JL, Raichle ME (2006) Spontaneous neuronal activity distinguishes human dorsal and ventral attention systems. Proc Natl Acad Sci USA 103:10046–10051

Fox MD, Zhang D, Snyder AZ, Raichle ME (2009) The global signal and observed anticorrelated resting state brain networks. J Neurophysiol 101:3270–3283

Greicius M (2008) Resting-state functional connectivity in neuropsychiatric disorders. Curr Opin Neurol 21:424–430

Guo WB, Liu F, Xue ZM, Xu XJ, Wu RR, Ma CQ, Wooderson SC, Tan CL, Sun XL, Chen JD, Liu ZN, Xiao CQ, Chen HF, Zhao JP (2012) Alterations of the amplitude of low-frequency fluctuations in treatment-resistant and treatment-response depression: a resting-state fMRI study. Prog Neuropsychopharmacol Biol Psychiatry 37:153–160

Guyon I, Elisseeff A (2003) An introduction to variable and feature selection. J Mach Learn Res 3:1157–1182

Guyon I, Weston J, Barnhill S, Vapnik V (2002) Gene selection for cancer classification using support vector machines. Mach Learn 46:389–422

Haller S, Lovblad KO, Giannakopoulos P, Van De Ville D (2014) Multivariate pattern recognition for diagnosis and prognosis in clinical neuroimaging: state of the art, current challenges and future trends. Brain Topogr 27:329–337

Hayasaka S, Laurienti PJ (2010) Comparison of characteristics between region-and voxel-based network analyses in resting-state fMRI data. Neuroimage 50:499–508

He Y, Wang J, Wang L, Chen ZJ, Yan C, Yang H, Tang H, Zhu C, Gong Q, Zang Y, Evans AC (2009) Uncovering intrinsic modular organization of spontaneous brain activity in humans. PLoS One 4:e5226

Hinrichs C, Singh V, Xu G, Johnson S (2009) MKL for robust multi-modality AD classification. In: Yang G-Z, et al. (eds) Medical image computing and computer-assisted intervention—MICCAI 2009. Springer, Berlin, pp 786–794

Jatzko A, Schmitt A, Demirakca T, Weimer E, Braus DF (2006) Disturbance in the neural circuitry underlying positive emotional processing in post-traumatic stress disorder (PTSD). An fMRI study. Eur Arch Psychiatry Clin Neurosci 256:112–114

Jin C, Qi R, Yin Y, Hu X, Duan L, Xu Q, Zhang Z, Zhong Y, Feng B, Xiang H, Gong Q, Liu Y, Lu G, Li L (2014) Abnormalities in whole-brain functional connectivity observed in treatment-naive post-traumatic stress disorder patients following an earthquake. Psychol Med 44:1927–1936

Kessler RC (2000) Posttraumatic stress disorder: the burden to the individual and to society. J Clin Psychiatry 61(Suppl 5):4–12 (discussion 13–14)

Kessler RC, Borges G, Walters EE (1999) Prevalence of and risk factors for lifetime suicide attempts in the National Comorbidity Survey. Arch Gen Psychiatry 56:617–626

Lanius RA, Williamson PC, Boksman K, Densmore M, Gupta M, Neufeld RW, Gati JS, Menon RS (2002) Brain activation during script-driven imagery induced dissociative responses in PTSD: a functional magnetic resonance imaging investigation. Biol Psychiatry 52:305–311

Lanius RA, Vermetten E, Loewenstein RJ, Brand B, Schmahl C, Bremner JD, Spiegel D (2010) Emotion modulation in PTSD:

clinical and neurobiological evidence for a dissociative subtype. Am J Psychiatry 167:640–647
Lindemer ER, Salat DH, Leritz EC, McGlinchey RE, Milberg WP (2013) Reduced cortical thickness with increased lifetime burden of PTSD in OEF/OIF Veterans and the impact of comorbid TBI. Neuroimage Clin 2:601–611
Linnman C, Zeffiro TA, Pitman RK, Milad MR (2011) An fMRI study of unconditioned responses in post-traumatic stress disorder. Biol Mood Anxiety Disord 1:8
Liu F, Guo W, Yu D, Gao Q, Gao K, Xue Z, Du H, Zhang J, Tan C, Liu Z, Zhao J, Chen H (2012a) Classification of different therapeutic responses of major depressive disorder with multivariate pattern analysis method based on structural MR scans. PLoS One 7:e40968
Liu F, Hu M, Wang S, Guo W, Zhao J, Li J, Xun G, Long Z, Zhang J, Wang Y, Zeng L, Gao Q, Wooderson SC, Chen J, Chen H (2012b) Abnormal regional spontaneous neural activity in first-episode, treatment-naive patients with late-life depression: a resting-state fMRI study. Prog Neuropsychopharmacol Biol Psychiatry 39:326–331
Liu F, Guo W, Fouche JP, Wang Y, Wang W, Ding J, Zeng L, Qiu C, Gong Q, Zhang W, Chen H (2013a) Multivariate classification of social anxiety disorder using whole brain functional connectivity. Brain Struct Funct. doi:10.1007/s00429-013-0641-4
Liu F, Guo W, Liu L, Long Z, Ma C, Xue Z, Wang Y, Li J, Hu M, Zhang J, Du H, Zeng L, Liu Z, Wooderson SC, Tan C, Zhao J, Chen H (2013b) Abnormal amplitude low-frequency oscillations in medication-naive, first-episode patients with major depressive disorder: a resting-state fMRI study. J Affect Disord 146:401–406
Liu F, Suk H-I, Wee C-Y, Chen H, Shen D (2013c) High-order graph matching based feature selection for Alzheimer's disease identification. In: Mori K, et al. (eds) Medical image computing and computer-assisted intervention—MICCAI 2013. Springer, Berlin, pp 311–318
Liu F, Wee CY, Chen H, Shen D (2014) Inter-modality relationship constrained multi-modality multi-task feature selection for Alzheimer's disease and mild cognitive impairment identification. Neuroimage 84:466–475
Long Z, Duan X, Xie B, Du H, Li R, Xu Q, Wei L, Zhang SX, Wu Y, Gao Q, Chen H (2013) Altered brain structural connectivity in post-traumatic stress disorder: a diffusion tensor imaging tractography study. J Affect Disord 150:798–806
Margulies DS, Vincent JL, Kelly C, Lohmann G, Uddin LQ, Biswal BB, Villringer A, Castellanos FX, Milham MP, Petrides M (2009) Precuneus shares intrinsic functional architecture in humans and monkeys. Proc Natl Acad Sci USA 106:20069–20074
Mega MS, Cummings JL, Salloway S, Malloy P (1997) The limbic system: an anatomic, phylogenetic, and clinical perspective. J Neuropsychiatry Clin Neurosci 9:315
Molina ME, Isoardi R, Prado MN, Bentolila S (2010) Basal cerebral glucose distribution in long-term post-traumatic stress disorder. World J Biol Psychiatry 11:493–501
Morey RA, Petty CM, Cooper DA, Labar KS, McCarthy G (2008) Neural systems for executive and emotional processing are modulated by symptoms of posttraumatic stress disorder in Iraq War veterans. Psychiatry Res 162:59–72
Mourao-Miranda J, Reinders A, Rocha-Rego V, Lappin J, Rondina J, Morgan C, Morgan K, Fearon P, Jones P, Doody G (2012) Individualized prediction of illness course at the first psychotic episode: a support vector machine MRI study. Psychol Med 42:1037
Murphy K, Birn RM, Handwerker DA, Jones TB, Bandettini PA (2009) The impact of global signal regression on resting state correlations: are anti-correlated networks introduced? Neuroimage 44:893–905
Power JD, Barnes KA, Snyder AZ, Schlaggar BL, Petersen SE (2012) Spurious but systematic correlations in functional connectivity MRI networks arise from subject motion. Neuroimage 59:2142–2154
Qin LD, Wang Z, Sun YW, Wan JQ, Su SS, Zhou Y, Xu JR (2012) A preliminary study of alterations in default network connectivity in post-traumatic stress disorder patients following recent trauma. Brain Res 1484:50–56
Rabinak CA, Angstadt M, Welsh RC, Kenndy AE, Lyubkin M, Martis B, Phan KL (2011) Altered amygdala resting-state functional connectivity in post-traumatic stress disorder. Front Psychiatry 2:62
Saad ZS, Gotts SJ, Murphy K, Chen G, Jo HJ, Martin A, Cox RW (2012) Trouble at rest: how correlation patterns and group differences become distorted after global signal regression. Brain Connect 2:25–32
Sato JR, Hoexter MQ, Fujita A, Rohde LA (2012) Evaluation of pattern recognition and feature extraction methods in ADHD prediction. Front Syst Neurosci 6:68
Satterthwaite TD, Wolf DH, Loughead J, Ruparel K, Elliott MA, Hakonarson H, Gur RC, Gur RE (2012) Impact of in-scanner head motion on multiple measures of functional connectivity: relevance for studies of neurodevelopment in youth. Neuroimage 60:623–632
Shaw ME, Moores KA, Clark RC, McFarlane AC, Strother SC, Bryant RA, Brown GC, Taylor JD (2009) Functional connectivity reveals inefficient working memory systems in post-traumatic stress disorder. Psychiatry Res 172:235–241
Shin LM, Rauch SL, Pitman RK (2006) Amygdala, medial prefrontal cortex, and hippocampal function in PTSD. Ann N Y Acad Sci 1071:67–79
Sokolova M, Japkowicz N, Szpakowicz S (2006) Beyond accuracy, F-score and ROC: a family of discriminant measures for performance evaluation. In: Sattar A, Kang BH (eds) Advances in artificial intelligence–AI2006. Springer, Berlin, pp 1015–1021
Sporns O (2011) The human connectome: a complex network. Ann N Y Acad Sci 1224:109–125
Suk HI, Lee SW, Shen D (2013) Latent feature representation with stacked auto-encoder for AD/MCI diagnosis. Brain Struct Funct. doi:10.1007/s00429-013-0687-3
Tuescher O, Protopopescu X, Pan H, Cloitre M, Butler T, Goldstein M, Root JC, Engelien A, Furman D, Silverman M, Yang Y, Gorman J, LeDoux J, Silbersweig D, Stern E (2011) Differential activity of subgenual cingulate and brainstem in panic disorder and PTSD. J Anxiety Disord 25:251–257
Tzourio-Mazoyer N, Landeau B, Papathanassiou D, Crivello F, Etard O, Delcroix N, Mazoyer B, Joliot M (2002) Automated anatomical labeling of activations in SPM using a macroscopic anatomical parcellation of the MNI MRI single-subject brain. Neuroimage 15:273–289
Uddin LQ, Kelly AM, Biswal BB, Castellanos FX, Milham MP (2009) Functional connectivity of default mode network components: correlation, anticorrelation, and causality. Hum Brain Mapp 30:625–637
van der Kolk BA (1989) Psychobiology of the trauma response. In: Lerer B, et al. (eds) New directions in affective disorders. Springer, Berlin, pp 443–446
Van Dijk KR, Sabuncu MR, Buckner RL (2012) The influence of head motion on intrinsic functional connectivity MRI. Neuroimage 59:431–438
Vincent JL, Patel GH, Fox MD, Snyder AZ, Baker JT, Van Essen DC, Zempel JM, Snyder LH, Corbetta M, Raichle ME (2007) Intrinsic functional architecture in the anaesthetized monkey brain. Nature 447:83–86
Wang J, Wang L, Zang Y, Yang H, Tang H, Gong Q, Chen Z, Zhu C, He Y (2009) Parcellation-dependent small-world brain

functional networks: a resting-state fMRI study. Hum Brain Mapp 30:1511–1523

Wang J, Zuo X, Dai Z, Xia M, Zhao Z, Zhao X, Jia J, Han Y, He Y (2013) Disrupted functional brain connectome in individuals at risk for Alzheimer's disease. Biol Psychiatry 73:472–481

Wee CY, Yap PT, Zhang D, Wang L, Shen D (2014) Group-constrained sparse fMRI connectivity modeling for mild cognitive impairment identification. Brain Struct Funct 219:641–656

Westman E, Aguilar C, Muehlboeck JS, Simmons A (2013) Regional magnetic resonance imaging measures for multivariate analysis in Alzheimer's disease and mild cognitive impairment. Brain Topogr 26:9–23

Xia M, Wang J, He Y (2013) BrainNet Viewer: a network visualization tool for human brain connectomics. PLoS One 8:e68910

Yan X, Brown AD, Lazar M, Cressman VL, Henn-Haase C, Neylan TC, Shalev A, Wolkowitz OM, Hamilton SP, Yehuda R, Sodickson DK, Weiner MW, Marmar CR (2013) Spontaneous brain activity in combat related PTSD. Neurosci Lett 547:1–5

Yehuda R, Flory JD (2007) Differentiating biological correlates of risk, PTSD, and resilience following trauma exposure. J Trauma Stress 20:435–447

Yin Y, Jin C, Eyler LT, Jin H, Hu X, Duan L, Zheng H, Feng B, Huang X, Shan B, Gong Q, Li L (2012) Altered regional homogeneity in post-traumatic stress disorder: a resting-state functional magnetic resonance imaging study. Neurosci Bull 28:541–549

Zalesky A, Fornito A, Harding IH, Cocchi L, Yucel M, Pantelis C, Bullmore ET (2010) Whole-brain anatomical networks: does the choice of nodes matter? Neuroimage 50:970–983

Zang YF, He Y, Zhu CZ, Cao QJ, Sui MQ, Liang M, Tian LX, Jiang TZ, Wang YF (2007) Altered baseline brain activity in children with ADHD revealed by resting-state functional MRI. Brain Dev 29:83–91

Zantvoord JB, Diehle J, Lindauer RJ (2013) Using neurobiological measures to predict and assess treatment outcome of psychotherapy in posttraumatic stress disorder: systematic review. Psychother Psychosom 82:142–151

Zeng L-L, Shen H, Liu L, Wang L, Li B, Fang P, Zhou Z, Li Y, Hu D (2012) Identifying major depression using whole-brain functional connectivity: a multivariate pattern analysis. Brain 135:1498–1507

Zeng L-L, Wang D, Fox MD, Sabuncu M, Hu D, Ge M, Buckner RL, Liu H (2014) Neurobiological basis of head motion in brain imaging. In: Proceedings of the national academy of sciences of the United States of America, vol 111, pp 6058–6062

Zuo XN, Di Martino A, Kelly C, Shehzad ZE, Gee DG, Klein DF, Castellanos FX, Biswal BB, Milham MP (2010) The oscillating brain: complex and reliable. Neuroimage 49:1432–1445